IMPACT PERFORMANCE AND AN EVALUATION CRITERION FOR MEDIAN BARRIERS

Hayes E. Ross, Jr., Texas Transportation Institute, Texas A&M University; and John F. Nixon, Texas State Department of Highways and Public Transportation

This study involves the determination of the impact performance of the Texas metal beam guard fence median barrier and a comparison of its performance with that of the Texas concrete median barrier. The metal beam guard fence consists of two standard W-shaped guardrails mounted back to back on a support post; the concrete barrier is a solid concrete barrier. The impact performance of the guard fence was determined from a combination of crash tests and from crash simulations by the Highway-Vehicle-Object Simulation Model. Standard-sized automobiles were used in both the crash tests and the crash simulations. A close comparison of test and simulated results verified the accuracy of the model in simulating impacts with the metal guard fence. The impact performance of the concrete barrier was obtained from another study. Inspection of 135 median barrier impacts on various urban freeways in Texas was made to determine the distribution of impact angles. These field measurements, supplemented by data from the highway simulation model, provided impact angle probabilities as a function of median widths. This study provides an evaluation criterion that can be used for objectively comparing the impact severity of the metal beam guard fence and the concrete median barrier as a function of the median's dimensions. The criterion is based on a design speed of 60 mph (97 km/h) and on impacts with a full-sized automobile.

•TO PREVENT median crossover accidents, the Texas State Department of Highways and Public Transportation (TSDHPT) uses, in most cases, two basic median barriers: the concrete median barrier (CMB) and the metal beam guard fence (MBGF). The CMB is for all practical purposes a rigid unyielding barrier; the MBGF is considered to be a flexible barrier, one that deforms on impact.

Several studies have been conducted to determine the impact performance of the CMB (1, 2, 3). It has been shown that for small impact angles the CMB can safely redirect an encroaching vehicle; however, these studies also showed that, as the impact angle increases, the impact severity increases considerably. Only limited impact performance data about MBGF existed before this study. One of the objectives of this study was therefore to determine the impact performance of MBGF so that objective comparisons could be made between the CMB and the MBGF. Crash tests and the Texas Transportation Institute version of the Highway-Vehicle-Object Simulation Model (HVOSM) computer program were used to accomplish this objective. The HVOSM was developed at Calspan Corporation for the Federal Highway Administration (9). Before applying the HVOSM, however, an extensive validation study was performed. Crash test data were compared with the HVOSM predictions. Some modifications were made to the HVOSM so that an acceptable comparison could be achieved.

This study also analyzed the relationship between median width and the probable angle of impact into a median barrier for errant vehicles. This relationship was needed to develop an evaluation criterion for the two barrier systems. It has been postulated that the CMB is best for narrow medians, where high impact angles are improbable, and that the MBGF should be used for wide medians. However, objective criteria to quantify what narrow and wide mean had to be developed. To accomplish this task, a combination of field measurements and HVOSM computer simulations was used.

TSDHPT personnel conducted the field measurements, and median barriers on selected urban freeways were inspected for impact damage. Where impacts had occurred, measurements of the angle of impact, median width, etc., were made. These data were then statistically analyzed to determine impact angle probabilities. The HVOSM was used to supplement the field data by defining upper limits on impact angles as a function of median widths.

This study result was an objective criterion that can be used in the median barrier selection process. The criterion, which is in the form of a graph, shows the relationship between impact severity and median width, on a probability basis, for the CMB and the MBGF. Other factors, such as installation and maintenance costs, must of course be considered in the selection process; however, an evaluation of these factors was not within the scope of this study. Full details of the study are given in a Texas Transportation Institute research report (10).

METAL BEAM GUARD FENCE BARRIER

Before the tests were conducted in this study, only one full-scale crash test had been conducted on the MBGF (2). In that test, an automobile impacted the barrier at 57.3 mph (92.2 km/h) at an impact angle of 25 deg. That test was denoted T4-1 (2) and will be referred to in the same way in this paper.

The impact conditions of two tests conducted in this study were 60 mph (97 km/h) at 8 deg, and 63.4 mph (101.4 km/h) at 14.7 deg. These two tests and the one mentioned above provided considerable insight concerning the impact performance of the MBGF for 60-mph (97-km/h) impacts. The tests also provided a data base from which the HVOSM could be validated. After validation, the HVOSM was used to determine the impact performance of the MBGF at speeds below and in excess of 60 mph (97 km/h).

Details

The as-tested MBGF (B)-74 barrier (TSDHPT designation) is shown in Figure 1. In some installations, a $\frac{3}{8}$-in. (9.5-mm) steel wire pedestrian control cable is placed below the guardrail. Also a headlight-barrier fence is sometimes placed on top of the barrier; however, it is assumed that neither of these features will significantly affect the impact performance of the barrier.

On impact, the MBGF support posts break away from their base, allowing the back-to-back guardrail to deform. The $\frac{3}{8}$-in. (9.5-mm) fillet welds connecting the outer faces of the two post flanges to the $\frac{5}{8}$-in. (15.9-mm) baseplate are designed to fracture at relatively low impact forces. Since the posts shear off at the base at a relatively low impact force, the rail does not rotate significantly; therefore, the possibility of vehicle ramping is minimized.

Crash Tests

The two crash tests conducted in the study are referred to as MB-1 and MB-2. The MB-1 test refers to the 60-mph (97-km/h), 8-deg impact, and the MB-2 test refers to the 63.4-mph (101.4-km/h), 14.7-deg impact.

Test Vehicles and Test Dummy

A 1965 Plymouth, weighing about 4,200 lb (1905 kg), was used in test MB-1. Figure 2 shows the vehicle before and after the test. A 1964 Plymouth, weighing approximately 4,200 lb (1905 kg), was used in test MB-2. Figure 3 shows the vehicle before and after the test. In each of the two tests a 50th percentile male dummy was placed in the driver's seat and lap belted.

Figure 1. Texas metal beam guard fence barrier, MBGF (B)-74.

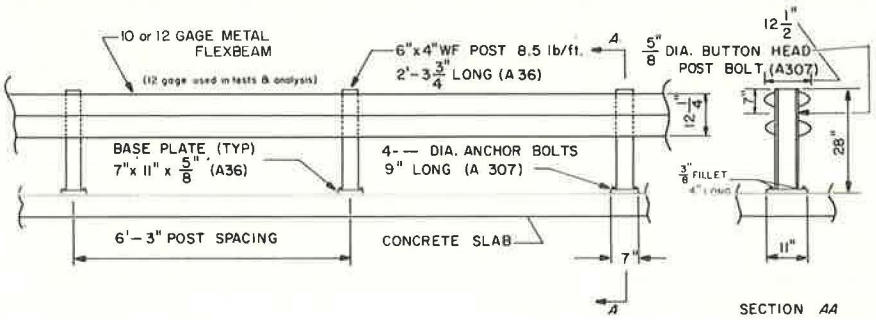

Figure 2. MB-1 test vehicle.

AFTER MB-1 TEST

AFTER MB-2 TEST

Data Acquisition

Crash test data were recorded by electronic instrumentation placed in the vehicle and by high-speed cameras that photographed the impacts. Three accelerometers were positioned near the center of gravity of the automobile. These accelerometers measured the longitudinal, lateral, and vertical accelerations, all with respect to a vehicle-fixed axis. The force in the dummy's lap belt during impact was measured. In addition, accelerometers were placed in the dummy's chest to measure accelerations in the fore and aft direction (eyeballs in or out) as well as in the left and right (lateral) direction. One high-speed camera was positioned with a field of view parallel to the longitudinal axis of the barrier, and the other camera's field of view was perpendicular to the barrier's longitudinal axis. Film speed was approximately 500 frames/sec. The film provided a time history of the vehicle's motion.

Test Results

The results of tests MB-1 and MB-2 are given in Table 1. Vertical accelerations were found to be small in comparison to the longitudinal and lateral accelerations and are therefore not shown. Damage to the MBGF after each test is shown in Figure 4. As can be seen, damage to the barrier after test MB-1 was negligible, and no repairs were necessary. Repairs to the barrier after test MB-2 would consist of replacing two 25-ft (7.5-m) W-beam guardrails, three support posts, and the necessary bolts, nuts, and so on. Damage to the automobile after each test is shown in Figures 3 and 4. The test car in MB-1 was still operable after the test; however, damage to the left front wheel assembly of the vehicle in test MB-2 prevented its operation after the impact.

VALIDATION OF MODEL FOR METAL BEAM GUARD FENCE IMPACT SIMULATIONS

The three full-scale crash tests described in the previous section provided impact performance data for the MBGF when impacted by a standard-sized automobile at about 60 mph (97 km/h); however, more data were desired concerning its performance since impacts in the field could be expected to occur at speeds both below and above 60 mph (97 km/h).

In lieu of additional crash tests (that were not within the budget), it was decided to determine if HVOSM could simulate an automobile impacting the MBGF. To make this determination, the three MBGF crash tests (MB-1, MB-2, and T4-1) were simulated by HVOSM, and the results were compared with the test results.

Process

The validation process actually involved a trial and error procedure. Errors were also uncovered in an impact subroutine of HVOSM, and these were corrected. Adjustments were made in the vehicle and barrier stiffness parameters until the HVOSM simulation converged on the results of the MB-2 test. However, these same stiffness parameters were used in the simulation of the other two tests (MB-1 and T4-1), and the resulting comparisons were very good. Except for the coefficient of friction between the vehicle and the barrier, parameters did not need to be adjusted in each test simulation. As a consequence, it was thought that these parameters could be used in HVOSM to simulate impacts with the MBGF at speeds above and below 60 mph (97 km/h). The value of the vehicle-barrier friction coefficient had to be adjusted upward as the angle of impact increased. This increase was necessary to simulate the effects of the slight pocketing that occurred, i.e., pocketing of the vehicle by the barrier.

Figure 3. MB-2 test vehicle.

BEFORE TEST

AFTER TEST

Table 1. Data from metal beam guard fence tests.

Item	Test Number MB-1	Test Number MB-2	Item	Test Number MB-1	Test Number MB-2
Vehicle			Departure angle, deg	4.0	3.8
Year	1965	1964	Departure speed, mph	47.0	52.0
Make	Plymouth	Plymouth	Accelerometer		
Weight, lb	4,200	4,200	Longitudinal		
Film			Peak, *g*	2.0[b], 5.3[c]	5.5[b], 5.4[c]
Impact speed, mph	60.0	63.4	Highest average, *g*[a]	0.03[b], 4.2[c]	0.90[b], 4.3[c]
Impact angle, deg	8.0	14.7	Lateral		
Dynamic barrier deflection, in.	1.0	12.0	Peak, *g*	5.3[b], 4.0[c]	7.0[b], 8.2[c]
			Highest average, *g*	3.2[b], 2.9[c]	4.7[b], 6.3[c]

Note: 1 lb = 0.45 kg, 1 mph = 1.6 km/h, 1 in. = 2.54 cm.
[a]Averaged over 50 msec. [b]Vehicle. [c]Dummy.

Figure 4. Metal beam guard fence damage.

BEFORE TEST

AFTER TEST

Comparisons Between Simulation and Test Results

Comparisons between HVOSM and the test results were made on two basic types of data: vehicle motion and accelerations at the vehicle's center of gravity.

Vehicle Motion

Figure 5 shows a comparison of test and simulation of vehicle motion for the MB-1 test [60 mph (97 km/h) and 8 deg]. Similar plots were made for the other two tests. The HVOSM perspective drawings were generated by a computer program (6) whose input is the HVOSM output. Hidden lines were removed from the perspective drawings by hand for clarity. The test photographs are prints made from selected high-speed film frames. The general motion of the HVOSM compares well with the test results. Note that the automobile does not roll appreciably after impact with the MBGF, as was the case in all three tests.

Acceleration

Figure 6 shows a comparison of test and simulation lateral acceleration for test MB-1. Similar comparisons were made for the other two tests. Comparisons were also made between test and simulation longitudinal accelerations. The HVOSM accelerations generally followed the trend of the test accelerations. In some instances test data were characterized by rapid changes, and HVOSM values were somewhat smoother. This high-frequency vibratory nature of the test data is attributed in part to ringing or high-frequency response of the sprung mass of the vehicle. HVOSM does not have the capability to simulate this type of response; however, the contribution of such accelerations to overall impact severity is not considered significant. Another reason for sudden and large changes in the test values is that, as the vehicle crushes, various members of various stiffnesses are encountered. HVOSM can simulate this effect to a small degree by hard points. A summary of the acceleration data is given in Table 2. Although some disparity occurs between test values and the HVOSM values for peak accelerations and the times at which these occur, the average accelerations reasonably agree. In most cases, more significance is placed on the highest average accelerations than on the highest peak accelerations. This is especially true when vehicle accelerations are used as a measure of severity (to the occupant or occupants of the vehicle).

After the validation efforts were evaluated, it was concluded that HVOSM (as modified) could be used to supplement crash test data for the MBGF. When the complex nature of the MBGF impacts was considered, the HVOSM predicted the gross motion of the vehicle and vehicle accelerations quite accurately.

PARAMETRIC STUDIES

Metal Beam Guard Fence

To supplement the MBGF crash test data, nine HVOSM simulations were made. Impacts at speeds of 50, 70, and 80 mph (80, 113, and 129 km/h) in combination with impact angles of 5, 15, and 25 deg were simulated. Table 3 gives the results of these nine simulations (runs 1 through 9). Also given in Table 3 are the results of the simulations of the three crash tests (runs 10, 11, and 12). The accelerations given in Table 3 are the highest average accelerations occurring over any 50-msec period. A small utility computer program was written to compute these maximum averages as well as the maximum severity index. The program scanned the data, computed the average accelerations and the severity index for all 50-msec periods, and selected and printed the maximums. The time period over which the maximum average longitudinal acceleration occurred did not necessarily correspond to that for the average lateral acceleration.

Figure 5. Test versus model vehicle motion, test MB-1.

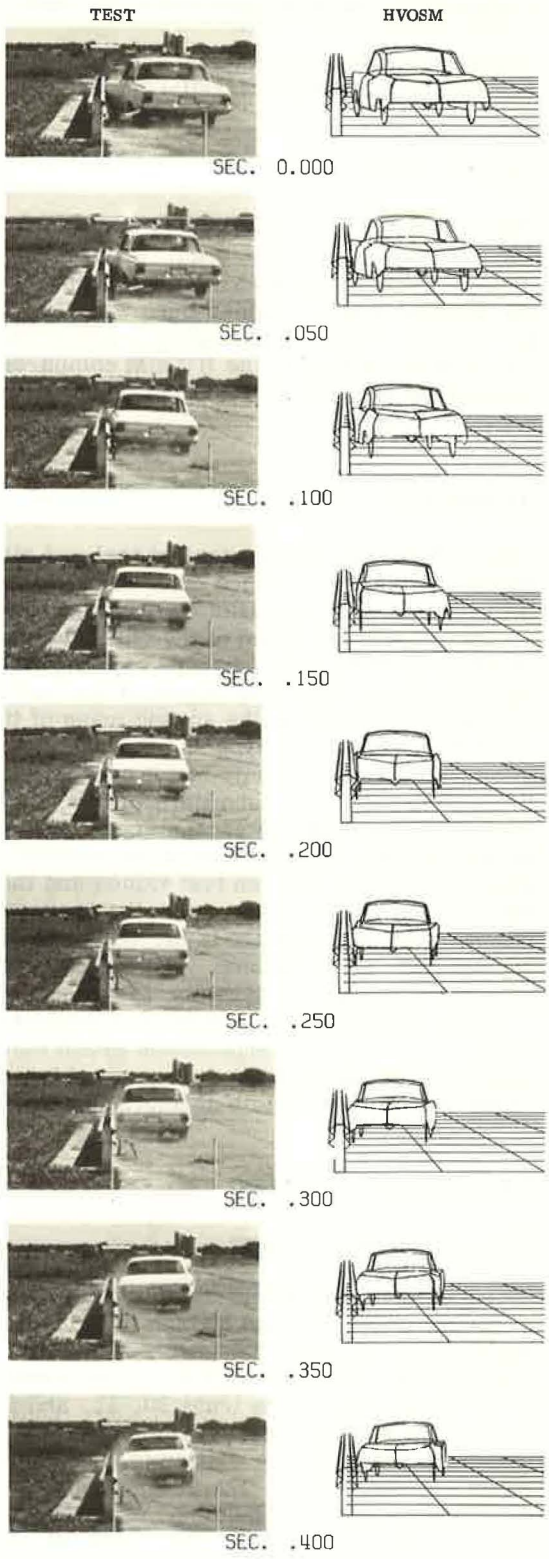

Figure 6. Lateral acceleration, test MB-1.

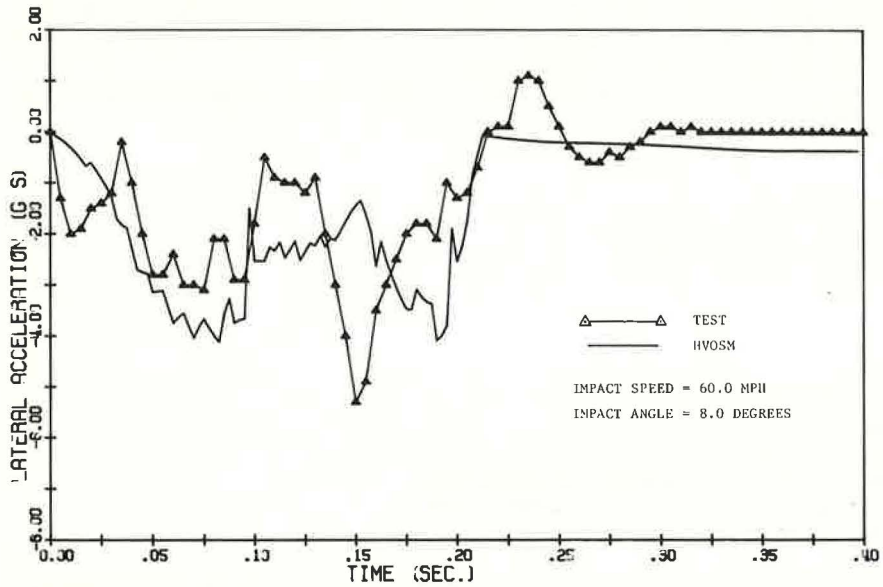

Table 2. Acceleration comparisons.

	Results (g/sec)					
	MB-1		MB-2		T4-1[a]	
Acceleration Type	Test	HVOSM	Test	HVOSM	Test	HVOSM
Peak lateral	5.3/0.16	4.1/0.19	7.0/0.070	6.2/0.113	—[b]	9.4/0.25
Peak longitudinal	2.8/0.08	1.4/0.07	5.0/0.080	2.8/0.058	12.0/0.13	11.0/0.103
Highest average lateral	3.2/0.14 to 0.19	3.6/0.045 to 0.095	4.7/0.17 to 0.22	4.8/0.173 to 0.223	—[b]	7.2/0.23 to 0.28
Highest average longitudinal	1.0/0.045 to 0.095	1.2/0.045 to 0.095	2.5/0.035 to 0.085	2.6/0.048 to 0.098	10.0/0.10 to 0.15	10.0/0.088 to 0.138

[a]Right frame member. [b]Not available.

Table 3. Parametric study results for metal beam guard fence and concrete median barrier.

		Impact Conditions		Exit	Max Roll	Max Avg Accelerations[b]			
Item	Run No.	Speed (mph)	Angle (deg)	Angle (deg)	Angle (deg)	g_{Long}	g_{Lat}	g_{Vert}	Max S.I.[c]
MBGF	1	50	5	1.9	1.8	0.56	1.92		0.39
	2	50	15	5.1	5.0	2.45	4.14		0.90
	3	50	25	12.2	9.6	7.80	5.50		1.57
	4	70	5	1.2	1.5	0.76	2.70		0.55
	5	70	15	2.9	2.3	2.87	5.51		1.15
	6	70	25	7.8	10.1	12.03	8.98		2.49
	7	80	5	1.0	1.6	0.88	3.15		0.64
	8	80	15	2.7	3.0	3.41	6.60		1.39
	9	80	25	7.0	9.7	15.30	11.53		3.17
	10	60	8	2.5	1.8	1.20	3.60		0.73
	11	63.4	14.7	3.6	5.0	2.59	4.80		0.98
	12	57.3	25.0	9.2	8.4	9.03	6.83		1.88
CMB	1	50.0	5.0	1.1	1.3	0.49	1.61	0.12	0.33
	2	70.0	5.0	0.3	2.2	0.72	2.53	0.43	0.52
	3	80.0	5.0	0.1	3.3	0.21	2.90	0.54	0.58
	4	50.0	10.0	2.5	4.2	1.13	2.99	0.94	0.64
	5	70.0	10.0	1.2	19.5	0.16	5.06	2.03	1.07
	6	80.0	10.0	1.2	34.6	1.92	6.42	2.61	1.38
	7	50.0	15.0	3.6	15.0	0.47	4.29	1.38	0.91
	8	70.0	15.0	—[d]	—[d]	2.81	6.44	3.16	—[d]
	9	80.0	15.0	—[d]	—[d]	3.24	7.49	3.29	—[d]
	10	50.0	25.0	—[e]	—[e]	4.45	7.41	4.28	1.76
	11	63.0	25.0	5.1	37.0	6.47	11.23	4.38	2.54
	12	70.0	25.0	—[e]	—[e]	9.37	12.27	1.78	2.81

Note: 1 mph = 1.6 km/h.

[a]When vehicle lost contact with barrier.
[b]Averaged over 50 msec at center of gravity. Maximum average longitudinal and lateral accelerations do not necessarily occur during the same time period.
[c]As computed over 50 msec.
[d]Vehicle rolled over on exiting from barrier. Severity was considered intolerable.
[e]Data unavailable.

In addition, the time period over which the maximum severity index occurred did not necessarily correspond to that for the maximum average longitudinal acceleration or to that of the maximum average lateral acceleration.

A severity index (SI) was used to quantify the severity (to an occupant) of the vehicle impacts with the MBGF. It is defined as follows (7):

$$SI = \sqrt{\left(\frac{G_{Long}}{G'_{Long}}\right)^2 + \left(\frac{G_{Lat}}{G'_{Lat}}\right)^2 + \left(\frac{G_{Vert}}{G'_{Vert}}\right)^2} \quad (1)$$

where

G_{Long} = average longitudinal acceleration,
G_{Lat} = average lateral acceleration,
G_{Vert} = average vertical acceleration,
G'_{Long} = tolerable average longitudinal acceleration,
G'_{Lat} = tolerable average lateral acceleration, and
G'_{Vert} = tolerable average vertical acceleration.

The terms in the numerator of equation 1 are the average accelerations of the vehicle, and the terms in the denominator are the limiting vehicle accelerations an occupant can withstand without serious or fatal injuries. It is assumed that SI > 1 indicates that an occupant would sustain serious or fatal injuries. A detailed description of the index is given in the literature (5, 6).

Limiting accelerations used in this study were as follows (7): $G'_{Long} = 7$, $G'_{Lat} = 5$, and $G'_{Vert} = 6$. For the MBGF, the vertical accelerations were negligible, and therefore only the first two terms of the SI were included. However, the severity indexes on the CMB involved all three terms since all three acceleration components were significant.

Concrete Median Barrier

The SI for the MBGF is compared with that of the CMB. Values of the SI for the CMB were obtained from a previous study (1), with two exceptions. For adequate comparison of the two barriers, two impacts had to be simulated with the CMBs that were not in the previous study. Impacts at 50 mph (80 km/h) and 25 deg and at 70 mph (113 km/h) and 25 deg were simulated. The results of these two runs, together with all other CMB data, are given in Table 3.

COMPARISON OF IMPACT PERFORMANCE OF CONCRETE MEDIAN BARRIER AND METAL BEAM GUARD FENCE

Impact Severity

SI versus impact speed for the CMB and the MBGF for three different impact angles is shown in Figure 7. Data in Figure 7 were taken from Table 3. For small impact angles, the two barriers are approximately equal in impact severity; however, as the impact angle increases, the difference in impact severity of the two barriers is more pronounced, and the MBGF provides the less severe impact. This result was expected since the MBGF does have flexibility and can dissipate a considerable amount of the energy of the impacting vehicle. The CMB is for all practical purposes a rigid barrier.

It can be seen in Table 3 that the MBGF can redirect a vehicle without introducing large roll angles, i.e., the potential for rollover appears to be minimal. This could be a significant factor when the MBGF and the CMB are compared since at high speeds and large impact angles the latter has shown a tendency to cause the impacting vehicle to roll over (1).

Damage Costs

Evaluation of the impact performance of a barrier should include consideration of repair costs to both the barrier and the vehicle. The following cost figures, which admittedly are based on limited data, give a quantitative measure of the damage costs incurred after impact with the MBGF and the CMB.

With regard to barrier damage, the CMB requires no repair for all practical purposes, at least for the impact conditions investigated. Damage to the MBGF for an impact at 60 mph (97 km/h) at 7 deg was negligible. Damage to the MBGF for 60-mph (97-km/h) impacts at 15 deg and 25 deg is approximately the same. Repair cost in these cases is based on previous estimates (2); a factor of 1.2 has been applied to estimate cost increases since those data were published. Estimated dollar costs to repair the barriers and the automobiles after impact with the respective barriers are as follows:

Impact Angle	Barrier	Vehicle
7-deg		
MBGF	Nil	490
CMB	Nil	615
15-deg		
MBGF	530	1,330
CMB	Nil	1,550
25-deg		
MBGF	530	1,430
CMB	Nil	1,500

Automobile repair costs were obtained in each case from a local automobile appraiser.

Based on the estimates and the corresponding impact conditions, impact with the CMB will cause more damage to the automobile than the MBGF. However, it is pointed out that, at impact angles of less than 7 deg, the CMB will redirect an automobile with little or no sheet metal damage; this reduces or eliminates damages. The MBGF does not have this capability, and some automobile damage can be expected for any impact.

IMPACT ANGLE PROBABILITIES

The study up to this point provided objective criteria for comparing the impact performance of the CMB and the MBGF for a given set of impact conditions, i.e., impact speed and angle. However, data in this form are of limited value if one cannot relate impact conditions (or probability thereof) to the particular median geometry in question. The objective of this phase of the study was therefore to determine the impact angle probability as a function of median width or the distance from the roadway to barrier's face. To accomplish this objective, the researchers relied on both field data and on data determined from the HVOSM. A description of each of these two approaches follows.

Field Data on Barrier Impacts

Valuable work on the nature of all vehicle encroachments has been done by Hutchinson and Kennedy (7); however, there was no apparent way to predict what number of these encroachments would have impacted a barrier, had there been one in the median, and at what impact angle this would have taken place. Therefore, a number of field evaluations were made to determine actual impact angles.

The field data were gathered by the research division of TSDHPT. The field sites

were urban freeways of several large cities in Texas. The collection procedure involved the location of sites where median barrier accidents had occurred (as judged by barrier damage) in which impact angles could be measured, either through skid marks or tire tracks. In some cases, the barrier deflection (permanent set) was measured; however, there was no attempt to relate barrier damage to any other parameters, such as vehicle speed.

Median widths investigated ranged from 13 to 56 ft (4 to 16.8 m), and 135 cases were recorded. However, a large portion of these (111) were in the 22 to 26-ft (6.7 to 7.9-m) median width range. In a few instances, the barrier was located on a raised median; in such cases a roll curb was used and, therefore, it is doubtful that it would have a significant effect on the vehicle's path, at least for the short distances between the curb and the barrier.

Inspections of impacts with barriers on narrow raised medians were also made by the TSDHPT. The following statement by D. Hustace of the department concerns this phase of the inspection:

> The narrow median, although sustaining numerous impacts, had frequently not provided tire tracks due to the airborne tire after having struck the curb face. Although curb scuff marks and barrier damage is usually readily apparent, the nearness of the barrier face and overhang of the vehicle would normally result in an over conservative angle from a calculated value. This factor, combined with the extreme hazard of angle measurements on narrow medians, leads me to feel that the data generated by Hutchinson and Kennedy for vehicle departure angles should be adequate to represent the narrow median situations since vehicle-driver recovery-response would be minimum due to the close proximity of the barrier. Also, in turn, the absence of wide median barrier sites and the lack of serious consideration for median barrier installations in the wide median does not demand the same urgent attention as does the barrier installation for the medium and narrow width medians.

A statistical analysis of the 135 cases led to the following conclusions:

1. There were enough data to determine a relation between impact angle and probability of occurrence for median widths between 22 and 26 ft (6.7 to 7.9 m). The relation is shown in Figure 8. The data from the 22, 24, and 26-ft (6.7, 7.3, and 7.9-m) medians were combined to develop this curve because there was not a significant variation in the distribution to warrant a curve for each of these four widths.
2. There were not enough data to develop distributions of impact angles as a function of median widths because most of the data were for median widths between 22 and 26 ft (6.7 and 7.9 m).
3. Based on the data for the 22 to 26-ft (6.7 to 7.9-m) medians, it appears that the distribution of impact angles for a given median width can be approximated by the normal distribution. The mean impact angle for the data was 10.8 deg with a standard deviation of 6.2 deg. It can be seen in Figure 8 that a normal distribution having a mean impact angle of 10.8 deg and a standard deviation of 6.2 deg correlates well with the field data.

Model Simulations of Encroachment Angles

A series of HVOSM runs were conducted to supplement the field data. The objective of these runs was to develop relationships between encroachment angle and median width for different probability levels. In the research approach, the HVOSM was used to establish extreme encroachment angles (95th percentile values) for any given median width. Further details of the procedure used to determine these angles are given later in the paper. Based on these extreme encroachment angles and assuming a zero impact angle at the 5th percentile, a normal distribution was constructed for various median widths (a normal distribution is uniquely defined, given any two points on the curve). Use of the normal distribution in this manner appears reasonable because of its close correlation with field data (Figure 8). From these data, curves were drawn depicting impact angle versus median width for different levels of probability. It is important to

note that the ability of the HVOSM to simulate an automobile during steering maneuvers has been demonstrated by other researchers (9).

Extreme Encroachment Angles

Much speculation has occurred concerning the highest angle at which an automobile can impact a barrier located a given distance from the roadway. This investigation did not provide data to end all speculations, nor did it purport to, but it did shed some light on the problem.

Basically, the HVOSM was used to determine the response and the encroachment angle of a standard automobile with standard tires as it was suddenly steered off the roadway while traveling at 60 mph (97 km/h). The automobile was assumed to be in a coast mode, i.e., with no traction after the steering maneuver began. The maneuver consisted of steering from a 0 steer angle to a prescribed angle in a prescribed time at a uniform rate. The turning rate was determined by observing the highest rates at which drivers had performed similar maneuvers in full-scale tests at the Texas Transportation Institute.

Four steering-angle limits were simulated in the HVOSM: 4, 8, 12, and 16 deg. The steer angle was increased to a selected limit at a constant rate and then held constant (most automobiles have a ratio of the steering wheel angle to steer angle of between 20 and 25). For example, an 8-deg steer angle would require between 160 and 200 deg of steering wheel turn.

A total of 12 simulation runs were made. For each of the four steering conditions described above, three tire-pavement friction coefficients were simulated, namely, 1.0, 0.75, and 0.5. The results were given in two basic forms: plots of the vehicle path and encroachment angle versus lateral distance. Figure 9 shows plots of the path of the center of gravity of the vehicle for a tire-pavement friction coefficient μ of 1.0 for the four steering angles. The lateral distance is a distance from the roadway tangent on which the steering maneuver began (roadway parallel to longitudinal distance axis). Note that an increase in the steer angle does not result in a proportionate increase in the path curvature, especially beyond steer angles of 8 deg. This is due primarily to the saturation of the side force capabilities of the front tires after the steer angle exceeds approximately 8 deg. It is conjectured that the curvature approaches a limiting value for steer angles of 16 deg. It is possible that other forms of steering input (e.g., nonlinear rates of steer application) could result in paths of larger curvature, but it is doubtful that the differences would be significant.

Also shown in Figure 9 is a path plot of the vehicle as simulated by a simple point mass model. It can be shown that the minimum radius r_{min} a point mass can follow is given by

$$r_{min} = \frac{v^2}{g\mu} \tag{2}$$

where

v = velocity of point mass,
μ = friction coefficient, and
g = gravitational acceleration.

From Figure 9, it can be seen that the actual paths (as determined by HVOSM) differ considerably from that of the point mass because of the inability of the point mass model to accurately represent the transient nature of vehicle handling. The point mass model assumes an instantaneous steady-state turn when the turn has been initiated, and the HVOSM accounts for the transient period of the vehicle's response.

Encroachment angles are shown in Figure 10 as a function of lateral distance. Coordinates of each of these curves were determined by computing the arc tangent of the

Figure 7. Severity index versus impact speed.

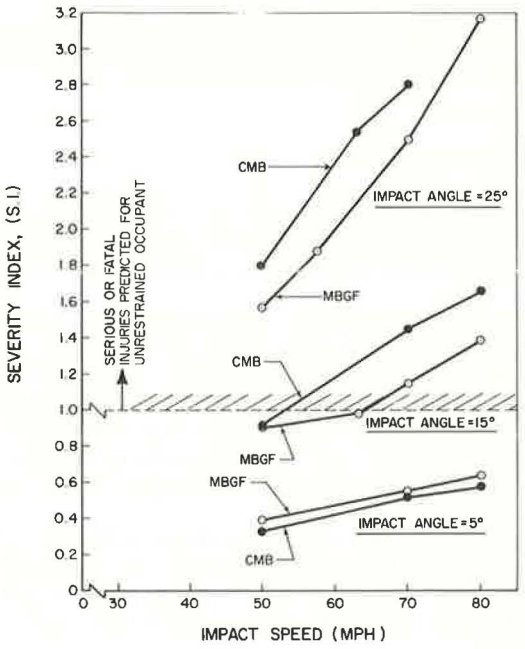

Figure 8. Distribution of impact angles for field data.

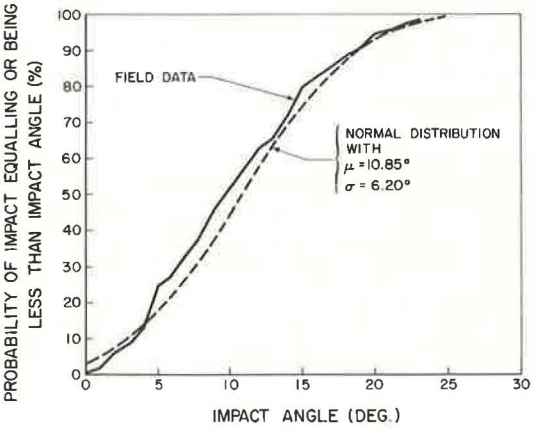

Figure 9. Vehicle path.

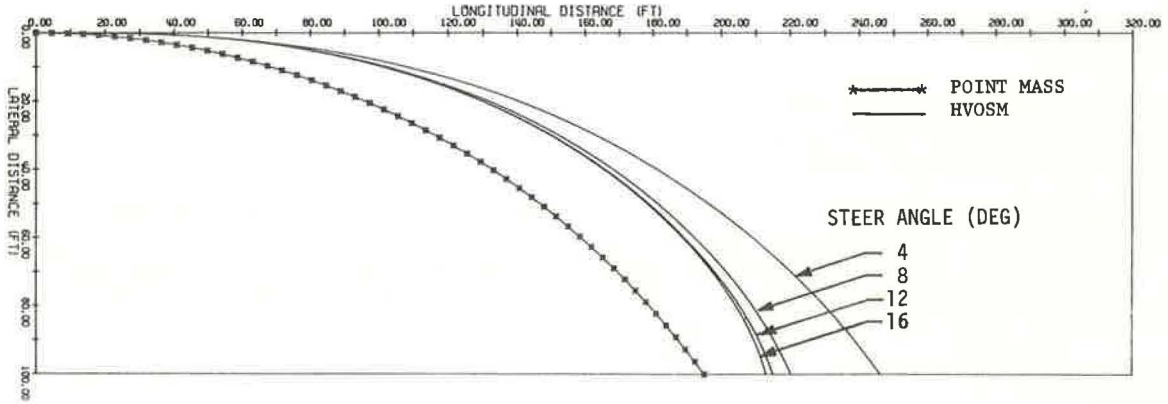

slope of the appropriate curve in Figure 9 as a function of lateral distance. The encroachment angle is the angle between a tangent to the center of gravity path and the roadway tangent.

Although the point mass model does not accurately simulate the vehicle's path, it does predict the encroachment angle quite accurately, at least for the extreme steering maneuvers simulated and for lateral distances up to about 40 ft (12 m). For lower friction coefficients, the comparison was found to be even better. In addition, many people felt that the point mass representation gave excessive encroachment angles; i.e., the vehicle could not attain the angles predicted by the point mass model. Such is not the case; in fact, for high skid-resistant pavements where large lateral distances are accessible, e.g., a wide median, the results indicate that the point mass predictions are too low.

For a relationship between extreme encroachment angle and median width (lateral distance), the values as determined for a steer angle of 16 deg and a friction coefficient of 1.0 were selected. In most cases these conditions would be extreme, and, as such, they represent what are considered to be limiting values.

Figure 11 shows the relationship between the extreme impact angle and the median distance D for two conditions: impact from lane 1 and impact from lane 2. Note that the median distance D is not the half-median width but rather is the distance from the edge of the roadway to the barrier face. It was assumed that the vehicle was in the center of the 12-ft (3.6-m) lane when the emergency steering maneuver began. The curves of Figure 11 were determined from Figure 10, and slight adjustments were made to account for the dimensions of a typical automobile (10, p. 59).

Note that the curve for the impact from lane 1 will intersect the vertical axis above zero for a zero median distance; i.e., there can be an impact angle even though there is no median distance because of the assumed 3-ft (0.9-m) gap between the vehicle and the face of the barrier for a vehicle traveling in the center of the lane.

Distribution of Probabilities

The probability distribution of impact angles for a given median distance was assumed to be a normal distribution. For determination of the distribution for a given median distance, the 95th percentile value of the impact angle was assumed to be that from the lane 1 curve of Figure 11, and the 5th percentile impact angle was assumed to be zero. These two points uniquely defined the distribution for any given median distance.

The decision to use these particular percentile values was arrived at through a trial and error procedure. Different combinations were tried, and the distributions were compared with the field data. Figure 12 shows that the predicted distribution (theoretical) compares reasonably well with the actual field data, for a median distance of 12 ft (3.6 m) [median width of about 24 ft (7.3 m)]. Although there are some differences in these two curves, the degree of correlation is considered to be good.

There are several factors that likely contributed to the differences that did occur in the curves of Figure 12. The first of these, and probably the most significant one, is the speed of the impacting vehicle. Unfortunately, there was no way to determine impact speeds from the field measurements. It is conjectured that the low-angle impacts occurred at speeds higher, on an average, than those of the higher angle impacts and that most of the impacts occurred at speeds of less than 60 mph (97 km/h). The theoretical distribution is based on an initial encroachment speed of 60 mph (97 km/h). Some slight decrease in speed occurred in the HVOSM simulations during the encroachment, but it was not considered significant [<2 mph (<3.2 km/h)].

Some of the barrier impacts likely occurred after the vehicle impacted another vehicle or object, and this could also cause differences. Actions of the driver during the encroachment, such as braking, could also have a significant effect on the vehicle's path. The number of lanes can also have an effect on the distribution of encroachment angles. Field data were taken on urban freeways with various numbers of lanes. As assumed, the theoretical distributions were based on encroachments from the inside

lane; however, the effect of the combination of these factors could be represented by the as-formulated theoretical distribution.

EVALUATION CRITERION

Impact performance data and impact angle data that were needed to formulate an evaluation criterion were now available. The criterion is based on a design speed of 60 mph (97 km/h) and relates to full-sized automobiles. Values of the severity index of barriers at 60 mph (97 km/h) as related to impact angle are given below:

Impact Angle (deg)	MBGF	CMB
5	0.47	0.42
15	0.96	1.18
25	2.00	2.39

These values are from Figure 7. The criterion is shown in Figure 13. Coordinates of the SI versus impact angle curves were taken from the table above, and the plots of median distance versus impact angle were determined from the assumed normal distributions.

The criterion referred to is based on safety considerations only, does not include cost and maintenance factors, and depends on the design speed. For example, if the design speed were 50 mph (80 km/h), the severity curves of Figure 13 for the two barriers would have been closer together. However, at lower design speeds, higher impact angles can be expected, and the impact angle distribution curves would have to be determined for the lower speeds.

Figure 13 allows one to objectively compare the impact severity of the two barriers as a function of the median distance. For example, assume that one is interested in the impact severities of the two barriers when they are placed 12.5 ft (3.7 m) from the roadway [a median width of approximately 25 ft (7.6 m)], for the 80th percentile impact. Application of the curves is as shown in Figure 13. The severity indexes were 0.90 for the MBGF and 1.09 for the CMB. These results indicate the MBGF to be about 21 percent less severe for the given conditions.

As mentioned previously, the selection process involves the consideration of other factors, such as initial and maintenance costs of the barrier and the hazard to repair crews and motorists while the barrier is being serviced. We think that a selection procedure based on a cost-effective analysis can be formulated that incorporates the effects of all these factors. Such a formulation, however, was not within the scope of this work.

The TSDHPT used the results of this study to establish guidelines for the selection of median barriers. These guidelines were also determined through careful consideration of other factors, such as maintenance costs, safety to maintenance crews who must repair the barriers, and the disruption of traffic during repairs. The guidelines are as follows (1 ft = 0.3 m):

Median Width (ft)	Barrier
<18	Concrete
18 to 24	Concrete or double steel beam
24 to 30	Double steel beam

Figure 10. Encroachment angles.

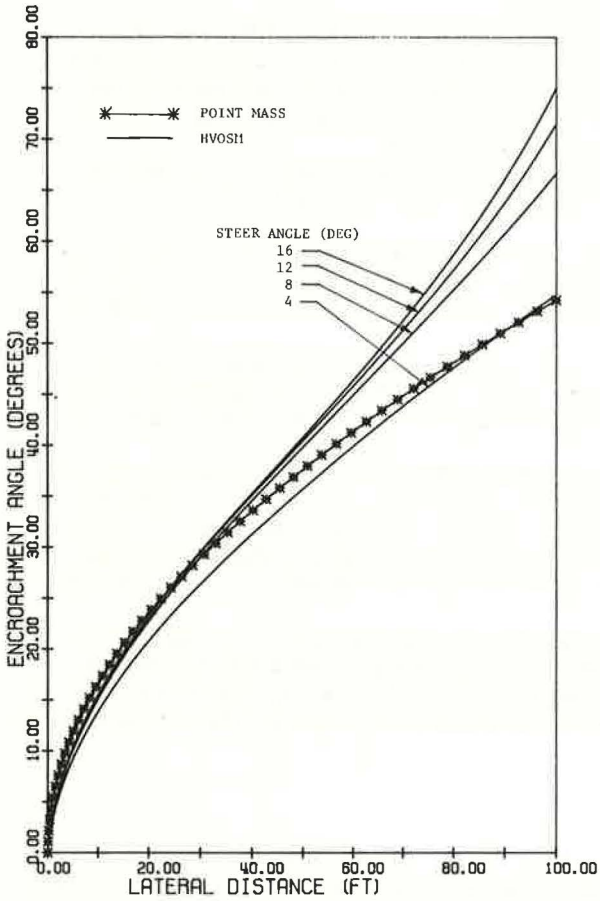

Figure 11. 95th percentile impact angle versus median distance.

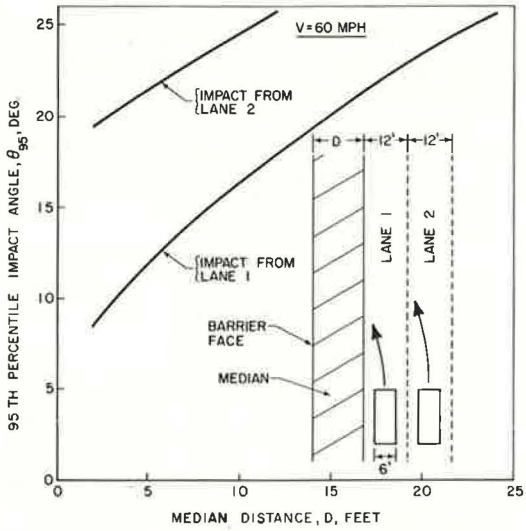

Figure 12. Impact angle versus probability of impact.

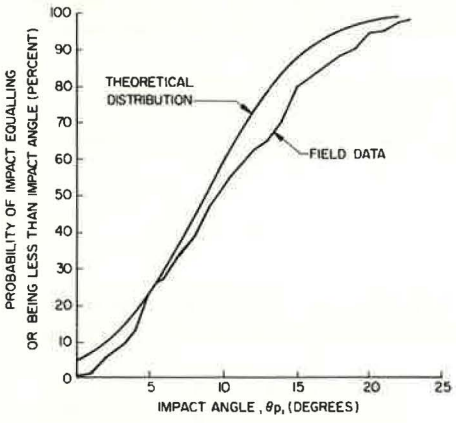

Figure 13. Selection criterion.

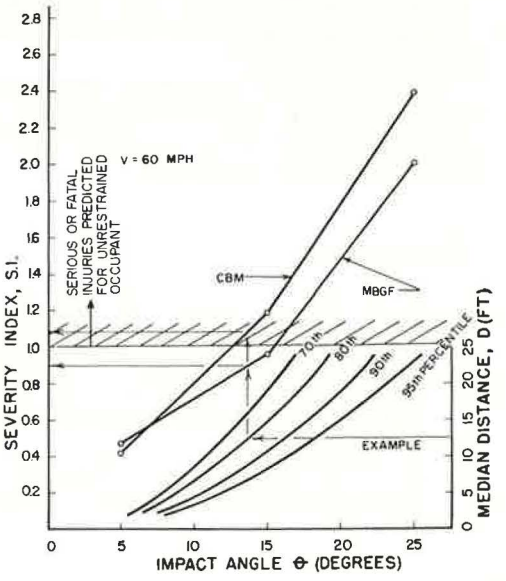

CONCLUSIONS

1. The Texas standard MBGF will contain and redirect an automobile impacting at 60 mph (97 km/h) at impact angles of 7, 15, and 25 deg. There is no tendency for the automobile to become unstable after impact with the MBGF, and the exit angle of the vehicle is not large. Serious or fatal injuries are not predicted for impacts at angles of less than 15 deg and speeds of less than 60 mph (97 km/h).
2. The as-modified version of the HVOSM can be used to simulate automobile impacts with the MBGF. Close correlations between test and simulated results form a basis for this conclusion.
3. The severity of impact with the Texas standard CMB at 60 mph (97 km/h) is approximately equal to that with the MBGF for impact angles of 7 deg or less. However, as the angle of impact increases, impacts become progressively more severe with the CMB than with the MBGF.
4. The CMB is practically maintenance free; repair of the MBGF after a 60-mph (97-km/h), 15-deg impact costs approximately $500. Based on gross estimates, automobile repair costs are slightly higher for a CMB impact than for an MBGF impact at 60 mph (97 km/h) and at 7 deg or more.
5. Sufficient field data were obtained to determine the percentile distribution of impact angles for a barrier placed in the center of a 24-ft (7.37-m) median. A theoretically derived distribution, obtained by application of the HVOSM, compared favorably with the field data. Percentile distributions of impact angles as a function of median distance (distance from roadway edge to barrier face) were obtained by the theoretical analysis.
6. An objective barrier evaluation criterion was developed from which the impact severity of the MBGF and the CMB can be determined for any given median distance. The criterion is based on a design speed of 60 mph (97 km/h) and impacts with a full-sized automobile. TSDHPT used this criterion to develop warrants for the use of these two barriers.

ACKNOWLEDGMENTS

This study was sponsored by the Texas State Department of Highways and Public Transportation in cooperation with the Federal Highway Administration. Several people provided valuable input to this study, for which we are appreciative. The guidance and suggestions of Dave Hustace of the department and Edward V. Kristaponis of FHWA are acknowledged. Field data on barrier impacts were collected and synthesized by Dave Hustace, Paul Tutt, and other members of Division 10 of the department. Larry Ringer of Texas A&M University provided guidance in the statistical analysis of the field data on barrier impacts.

The contents of this paper reflect the views of the authors, who are responsible for the facts and the accuracy of the data presented. The contents do not necessarily reflect the official views or policies of FHWA. This paper does not constitute a standard, specification, or regulation.

REFERENCES

1. R. D. Young, E. R. Post, and H. E. Ross, Jr. Simulation of Vehicle Impact With Texas Concrete Median Barrier: Test Comparisons and Parameter Study. Highway Research Record 460, 1973, pp. 61-72.
2. E. R. Post, T. J. Hirsch, G. G. Hayes, and J. F. Nixon. Vehicle Crash Test and Evaluation of Median Barriers for Texas Highways. Highway Research Record 460, 1973, pp. 97-113.
3. L. C. Lundstrom, P. C. Skeels, B. R. Englund, and R. A. Rogers. A Bridge Parapet Designed for Safety. Highway Research Record 83, 1965, pp. 169-183.

4. C. M. Theiss. Perspective Picture Output for Automobile Dynamic Simulation. Cornell Aeronautical Laboratory, CAL Rept. VJ-2251-V-2R, Dec. 1968.
5. G. D. Weaver and E. L. Marquis. The Relation of Side Slope Design to Highway Safety (Combination of Slopes). Texas Transportation Institute, Texas A&M Univ., Rept. RF 626B, Oct. 1973.
6. H. E. Ross, Jr., and E. R. Post. Criteria for Guardrail Need and Location on Embankments. Texas Transportation Institute, Texas A&M Univ., Research Rept. 140-4, Vol. 1, April 1972.
7. J. W. Hutchinson and T. W. Kennedy. Medians of Divided Highways—Frequency and Nature of Vehicle Encroachments. Engineering Experiment Station, Univ. of Illinois, Bulletin 487, 1966.
8. S. M. Selby. Standard Mathematical Tables. Chemical Rubber Co., 17th Ed., 1969, pp. 581-588.
9. R. R. McHenry and N. J. Deleys. Vehicle Dynamics in Single-Vehicle Accidents—Validation and Extension of the Computer Simulation. Cornell Aeronautical Laboratory, CAL Rept. VJ-2251-V-3, Dec. 1968.
10. H. E. Ross, Jr. Impact Performance and a Selection Criterion for Texas Median Barriers. Texas Transportation Institute, Texas A&M Univ., Research Rept. 140-8, April 1974.